

Titanium Implant Surface Modification in Physiological Serum Containing New Mixed Inhibitor Based on Poly(vinyl) Alcohol/Silver Nanoparticles/Epirubicin

Adriana Samide^{1*}, Simona Iordache¹, Gabriela Eugenia Iacobescu², Cristian Tigae¹, Cezar Spînu¹

¹ University of Craiova, Faculty of Sciences, Department of Chemistry, 107i Calea Bucuresti, Craiova, Romania

² University of Craiova, Faculty of Sciences, Department of Physics, A.I. Cuza, no.13, Craiova, Romania

*E-mail: samide_adriana@yahoo.com

Received: 25 August 2018 / Accepted: 1 October 2018 / Published: 5 November 2018

The titanium behaviour in physiological serum blank (PS) and containing silver nanoparticles (nAg) and polyvinyl alcohol (PVA) in the absence and presence of epirubicin cytostatic (EPR) was studied by potentiodynamic polarization and electrochemical impedance/admittance spectroscopy. These showed that the electrochemical parameters classically ranged, meaning that the addition of nAg/PVA and epirubicin in physiological serum leads to corrosion current density decline and polarization resistance increase while the conductance is diminished. The induced modifications on titanium surface were highlighted by optical microscopy and atomic force microscopy (AFM) which displayed the specific coating adsorbed on titanium surface. Consequently, nAg/PVA improves the epirubicin effect on titanium surface. Prior to the measurements above mentioned, the interactions between nAg and PVA were studied, showing the nAg/PVA composite formation. Also, the interactions between Cl⁻ ions, epirubicin and nAg were discussed, in order to better understand the influence of nAg/PVA composite on the epirubicin protective performance on the titanium surface.

Keywords: titanium bioimplant; silver nanoparticles/poly(vinyl) alcohol composite; epirubicin cytostatic; electrochemical measurements; AFM

1. INTRODUCTION

The cytostatics are drugs used to block the growth of cancer cells by influencing cellular metabolism, thus the cell division and reproduction being inhibited. The cytostatics are classified according to their action mechanisms and attack zones. These, generally, are toxic substances with many effects, sometimes dramatic, on the human body, especially in the early days after administration [1-6]. Epirubicin is an anthracycline drug with the molecular mass of 543 g mol⁻¹, delivering to

patients in limited doses, because it does not hold the ability to target just tumors, it being partially distributed in healthy tissues [7]. The intelligent systems for controlled drug delivery to diseased cells could be achieved by designing of some polymer-drug systems [7].

Poly(vinyl) alcohol (PVA) is a water soluble synthetic polymer with the formula $[-\text{CH}_2\text{CH}(\text{OH})-]_n$ that is commercialized as granules or powder. It is used in ceramics and paper industry, in cosmetic or medicine. Additionally, it can be suitable for polymeric film formation by its adsorption on the metal surfaces as single compound or doped with different particles constituting especially a favorable matrix for silver nanoparticles [8-11]. In order to obtain the composites based on polyvinyl alcohol and Ag nanoparticles as fibers, gels or thin films [11], different techniques were employed, one of which being the electrochemical synthesis [8].

The polymer-drug systems can interact with metals/alloys leading to improve the surface characteristics. As it is known, titanium has many applications due to favorable properties such as, corrosion resistance, thermal conductivity, mechanical processability and malleability, being used as implant material due to its biocompatibility and ability to osseointegrate in host bone tissue [12-14].

The bioimplant exposure in the human body environment leads to the appearance of corrosion processes followed by its wear, thus affecting the metal/tissue interface. Moreover, due to oxidation/corrosion, the nearby tissue of the implant can be infested with certain products that can cause undesirable local reactions followed by some cytotoxic and allergenic effects on the body and finally leading to implant failure [15]. The studies were focused on the development of some tissue-compatible and clinically available inorganic and organic coatings, improving the osteoblast functions [13, 14]. The coatings also retard the wear and corrosion effects such as the release of metallic cations in the body physiological medium which affect its natural functionality but improve biocompatibility and antimicrobial activity [16].

Generally, the investigation of layers adsorbed on different substrates was carried out by employing the surface characterization techniques, such as: Mössbauer spectroscopy [17-19], X-ray Photoelectron Spectroscopy (XPS) [20, 21] Scanning Electron Microscopy (SEM) [22-27], Atomic Force Microscopy [28, 29] or optical microscopy [17, 30-32]. The deposited layers on titanium such as, carbonitride (TiCN) coating [33] and TiO_2 thin film [34] were analyzed by Auger electron spectroscopy [33], X-ray diffraction (XRD) [34] and XPS [33, 34], their morphology being examined by AFM [33, 34]. Assembling of the coatings based on polymer-drug systems could be a good way to optimize the metal/tissue interface. The possible prophylactic or sometimes therapeutic features of incorporated drug in layer help the tissue to heal more quickly. In this regard it is very difficult to make some presumptions the more so as, in the medical world are numerous controversies, especially if regarding the cytostatics.

The main objective of the current study is to investigate the protective performance of a polymer-nanoparticles-drug coating adsorbed on the titanium surface in physiological serum (PS) employing electrochemical measurements followed by titanium surface characterization through optical microscopy and atomic force microscopy (AFM). Thus, silver nanoparticles (nAg) were dispersed in a 0.1% polyvinyl alcohol solution (PVA) obtaining a nanodispersion containing the nAg/PVA composite. Finally, the titanium behaviour was tested in four environments: (1) physiological serum (PS); (2) physiological serum containing nAg/PVA composite referred further

with the abbreviation “SPS”; (3) physiological serum (PS) containing epirubicin (PS/EPR); (4) physiological serum (PS) containing nAg/PVA and epirubicin (SPS/EPR). The interaction between nAg, epirubicin and Cl^- ions was discussed.

2. MATERIALS AND METHODS

2.1. Materials

The titanium plates (active area of 1.0 cm^2) with the purity of about 99.9% (Sigma Aldrich product) were sanded, washed, degreased with acetone and dried in warm air and then, these were submitted to corrosion in physiological serum (solution of 0.9% NaCl) without and with poly(vinyl) alcohol, silver nanoparticles and epirubicin. The epirubicin was purchased from SC Actavis SRL, Romania, being bottled in vials of 50 mL, in a concentration of 2.0 mg mL^{-1} , the poly(vinyl) alcohol and silver nanopowder being purchased from Sigma Aldrich.

The nanodispersion of silver nanoparticles in polyvinyl alcohol was prepared as follows: (i) a 0.1% polyvinyl alcohol solution was prepared; (ii) 500 mg L^{-1} silver nanoparticles were added and kept under stirring for 120.0 minutes; (iii) samples were taken at certain time intervals to undergo spectrophotometric analysis; (iv) after 85.0 minutes the absorbance maximum remained roughly the same, indicating that the maximal dispersion threshold of the silver nanoparticles in the polyvinyl alcohol solution was reached; (v) the excess of nanoparticles were filtered and a very fine yellow nanodispersion with a seemingly homogeneous appearance was obtained; (vi) its concentration was computed using the calibration curve equation previously determined, namely: $y = 0.0245x - 0.0062$.

The stability of the nanodispersion was verified over time and it was found that the absorbance maximum remained the same after 48 hours; no deposition or the initial appearance change was observed, indicating that the equilibrium between non-adsorbed/adsorbed silver nanoparticlae on PVA molecular chain was reached. The relative adsorption capacity (q) expressed as $[\text{mg (nAg)/g PVA}]$ was calculated obtaining the maximum adsorption capacity, $q_{\text{max}} = 281 \text{ mg/g}$ (before filtration) and the equilibrium adsorption capacity, $q_e = 212 \text{ mg/g}$ corresponding to the stable nanodispersion obtained after filtration.

Consequently, the corrosion was induced to titanium, in the environments presented below. Also, the short abbreviations are referred next.

1. Titanium induced corrosion in physiological serum blank (Ti/PS).
2. Titanium induced corrosion in physiological serum containing 212 mg L^{-1} nAg/0.1% PVA nanoparticles (Ti/SPS).
3. Titanium induced corrosion in physiological serum containing 0.018 mol L^{-1} epirubicin (Ti/EPR).
4. Titanium induced corrosion in physiological serum containing 212 mg L^{-1} nAg/0.1% PVA and 0.018 mol L^{-1} epirubicin (Ti/SPS/EPR).

2.2. Electrochemical measurements

As mentioned in previous studies [21, 22, 26, 28-30, 35], the electrochemical measurements were performed using a potentiostat/galvanostat, VoltaLab with VoltaMaster 4 software using a standard electrochemical cell with three electrodes: working electrode (titanium, active area 1.0 cm^2), auxiliary electrode (platinum, area of 1.0 cm^2) and Ag/AgCl, as reference electrode. The potentiodynamic polarization was carried out at room temperature, in the potential range from -800.0 mV to 800 mV , with a scan rate of 1.0 mV s^{-1} , after pre-polarization of electrodes at open circuit, time of 4.0 minutes. The potentiodynamic curves were processed as semilogarithmic curves, in the potential range of $\pm 250.0 \text{ mV}$ vs. corrosion potential and as a linear diagram in the potential domain close to corrosion potential, $\pm 20 \text{ mV}$. The electrochemical impedance spectroscopy was performed after the potentiodynamic polarization, in the frequency range between 10^{-1} Hz and 10^5 Hz , with current amplitude, AC of 10 mV , the relaxation time of the electrodes at open circuit being 4.0 minutes. The Nyquist_impedance and Nyquist_admittance plots were recorded.

2.3. UV-Vis spectrophotometry

The UV-Vis spectra were recorded in wavelength range between 800.0 nm and 200.0 nm for the following environments: (1) – 0.1 % PVA solution containing 500.0 mg L^{-1} silver nanoparticles at some time intervals: 5.0 min., 10.0 min., 20.0 min., 30.0 min., 40.0 min., 50.0 min., 60.0 min., 70.0 min., 85.0 min., 105.0 min., 120.0 min.; (2) – nAg/PVA nanodispersion, after filtration; (3) nAg/PVA in physiological serum (SPS, with the composition: 212 mg L^{-1} nAg, 0.1 % PVA and 0.9% NaCl); (3) – $1.8 \cdot 10^{-5} \text{ mol L}^{-1}$ (0.018 mM) epirubicin in physiological serum (PS/EPR); (4) – $1.8 \cdot 10^{-5} \text{ mol L}^{-1}$ epirubicin in SPS (SPS/EPR). The molecular structure and optimization formula of epirubicin are presented in Figure 1. The Varian Cary 50 spectrophotometer with CaryWin software was used, as reported in previous studies [35-37].

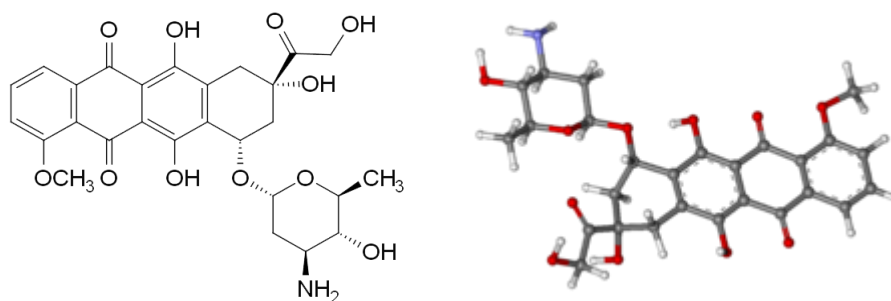


Figure 1. The molecular structure and optimized formula of epirubicin

2.4. Surface characterization

The titanium surface morphology was discussed based on optical microscopy and atomic force microscopy (AFM) images, acquiring the microscopic slides of standard titanium and corroded

samples: Ti/PS; Ti/SPS; Ti/PS/EPR; Ti/SPS/EPR. The optical images for all titanium samples, were designed with the metallographic Euromex microscope [30, 32] and the AFM was performed using “non-contact mode atomic force microscopy (NC-AFM, PARK XE-100 SPM system)” - as described in detail in our previous studies [28, 29].

3. RESULTS AND DISCUSSION

3.1. The characterization of tested inhibitors by UV-Vis spectrophotometry

The UV-Vis spectra were recorded at certain time intervals until a constant absorbance over time was obtained, implying that the dispersion limit concentration of nanoparticles in the PVA solution was reached. Figure 2a illustrates the UV-Vis spectra recorded for the nAg/PVA dispersion, time of 120 minutes. The absorbance maximum at 409.0 nm corresponds to silver nanoparticles [36-38], the absorption band is relatively symmetrical indicating that the medium does not contain many agglomerated nanoparticles [36]. A similar spectrum for Ag/PVA has been reported in other studies [36].

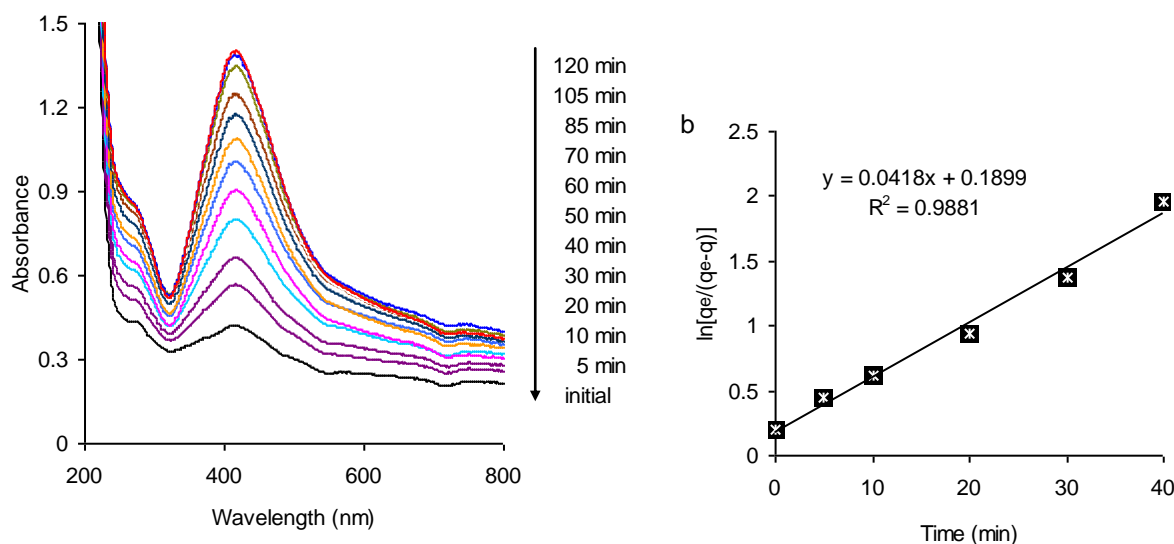


Figure 2. UV-Vis spectra recorded for nAg/PVA at room temperature (a); the pseudo-first order kinetic model approached for the nAg/PVA (b)

Large bands with an adsorption shoulder at greater wavelengths are observed, probably due to the nAg randomly dispersion in the polymer matrix [38], depending on the size of aggregates which appeared by agglomeration of nanoparticles. Some studies have reported that the silver nanoparticles are adsorbed on PVA macromolecular chain through Van der Waals [39] and/or Ag-O bonds [40], forming a nAg/PVA composite type [41]. As shown in Figure 2a, the dispersion capacity into aqueous phase is time dependent. After 85 minutes, the spectra overlap what indicates over-saturation and reaching the threshold of nAg dispersion.

The adsorption dynamics of the nAg on PVA molecular chain was good fitted by the Lagergren model of pseudo-first order, representing by Equation 1 [42, 43].

$$\ln \frac{q_e}{q_e - q} = kt \quad (1)$$

where q_e and q are the adsorption capacity (mg/g) at equilibrium, and at time “t”, respectively; k represents the rate constant of pseudo first-order adsorption.

As shown in Section 2.1, the nAg concentration, at different times, was computed using the calibration curve equation and the relative adsorption capacity (q) was determined as [mg (nAg)/g PVA], obtaining for q_e a value of 212 mg/g. According to the Equation 1, the graph $\ln [q_e/(q_e-q)]$ vs. time (Fig. 2b) represents a straight line with the slope dy/dx assigned to the rate constant (k) that reached a value of 0.0418 min^{-1} . Consequently, the macromolecular chain of PVA represents a vehicle/adduct for silver nanoparticles leading to aqueous nanodispersions with a seemingly homogeneous appearance which can be applied in various fields.

To better understand the action mechanism of a mixed inhibitor based on polyvinyl alcohol, silver nanoparticles and epirubicin, their interactions in the absence and presence of physiological serum (Cl^- ions) were studied.

Figure 3 displays the UV-Vis spectra of silver nanodispersion in 0.1% PVA and in physiological serum (PS) in the absence and presence of epirubicin (EPR).

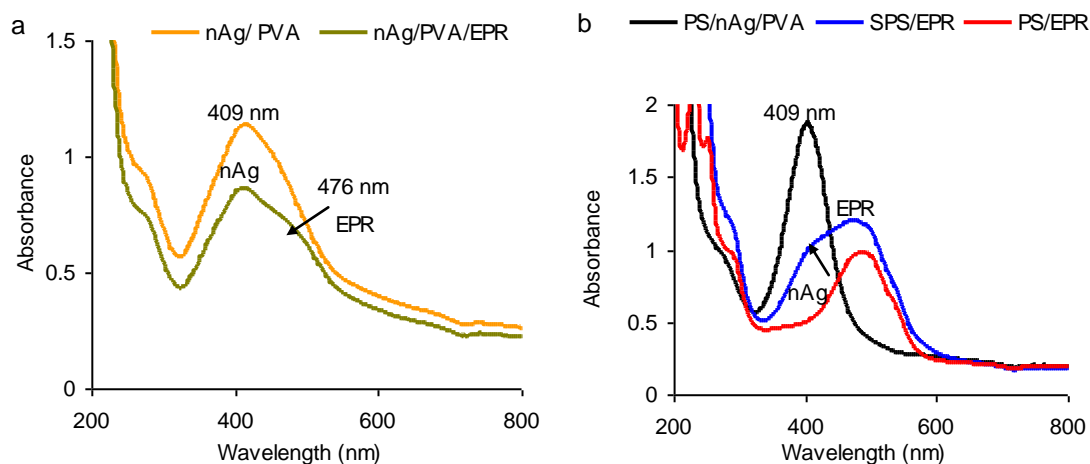


Figure 3. UV-Vis spectra of nAg and EPR recorded in: a – 0.1% PVA solution; b –Physiological serum containing the tested inhibitors

As shown Figure 3a, in the cytostatic presence (nAg/PVA/EPR spectrum), the nAg absorbance maximum declines and a large shoulder centered to 476.0 nm can be observed, it being assigned to epirubicin [44]. The significant change of absorption peak characteristics reveals more than just a simple interference, it could also suggest, the appearance of an interaction between nAg and EPR (Fig. 3a - nAg/PVA spectrum). In physiological serum (Fig. 3b), the epirubicin spectrum (PS/EPR spectrum) indicates an absorption maximum at 478.0 nm and completely different characteristics in the presence of nAg/PVA (SPS/EPR spectrum). The almost Gaussian shape of PS/nAg/PVA spectrum suggests an evenly distribution of silver nanoparticles in the PVA solution, in the presence of Cl^- ions compared to that displayed in their absence (nAg/PVA spectrum from Fig. 3a). As shown in Figure 3b,

in the presence of Cl^- ions, the EPR peak (SPS/EPR spectrum) is better highlighted compared to the one recorded in their absence (nAg/PVA/EPR spectrum from Fig. 3a). Also, the nAg peak is drastically changed compared to that obtained for silver nanoparticles in physiological serum (PS/nAg/PVA spectrum from Fig. 3b) as well as in the absence of Cl^- ions (Fig. 3a).

Thus, strong interactions occur, probably due to the fact that the epirubicin molecules envelop the silver nanoparticles, creating the “so-called cage effect” and thus the PVA macromolecule becomes a vehicle for aggregates type of nAg/EPR.

3.2. Potentiodynamic polarization

The potentiodynamic measurements were performed in order to induce some changes on the titanium surface in contact with the physiological serum (PS) and the complex system containing silver nanoparticles and poly(vinyl) alcohol in physiological serum, the nAg/PVA/PS system (SPS) both without and with epirubicin. The potentiodynamic polarization results are presented in Figure 4.

Distinctive potentiodynamic curves can be observed in Fig. 4a. The titanium curve in PS blank (1) indicates two passive domains, in potential range of -400.0 mV and -200.0 mV and between 400.0 mV and 800.0 mV interrupted by an active area from -200.0 to 400.0 mV, indicating a surface instability due to the formation of titanium compounds which develop a weakly anchored layer on substrate. The titanium curve characteristics in STS (2) is shifted in the lower current area, the current density increases proportionally with the potential, probably due to the silver oxidation process which prevails of the titanium one. In the presence of EPR, the Ti-curve shape in PS (3) changes, between -400.0 mV and 400.0 mV, the current density increases insignificantly with the potential increase, indicating the formation of a surface protective layer *via* EPR adsorption. The last Ti-assigned curve in STS (4) indicates an extended passivity range from $E(i = 0)$ to 400.0 mV showing that nAg/PVA enhances the EPR effect, behaving as a vehicle that facilitates EPR diffusion at the metal/electrolyte interface.

The semilogarithmic curves (Fig. 4b) show that the corrosion potential (E_{corr}) moves to higher values and the anodic and cathodic processes are influenced in a considerable manner, in all cases, compared to that associated to titanium in PS blank (1). In the present nAg/PVA in PS (2) the curve is shifted to a higher potential area, but remains at about the same level of current densities as the one obtained for titanium in PS. This suggests a slightly protection of the titanium surface most likely due to a physical adsorption of PVA through free HO^- groups without the formation of a metal-metal bond, thus being facilitated the primary oxidation of the silver adsorbed on the PVA macromolecular chain. Epirubicin in PS (3) classically behaves like an inhibitor that acts by adsorption on the surface forming a protective film that retards titanium corrosion. EPR in STS (4) acts almost similarly, indicating that nAg/PVA is more a transporter than a synergistic inhibitor. Similar curves were obtained for pure titanium corrosion in sulfuric acid solution in the presence of Cl^- ions [45], which can disturb the titanium spontaneous passivation state. Another study showed that the PVA addition in physiological serum led to the protective coating formation by inhibitor adsorption on the titanium surface due to the polar effect of hydroxyl groups [46].

The same conclusions can be drawn from the linear diagram (Fig. 4c) obtained in the potential area close to the corrosion potential where the i vs. E plot is a straight line, with the slope $(di/dE)_{E \rightarrow E_{corr}}$ corresponding to the polarization conductance (C_p) [28, 29, 47].

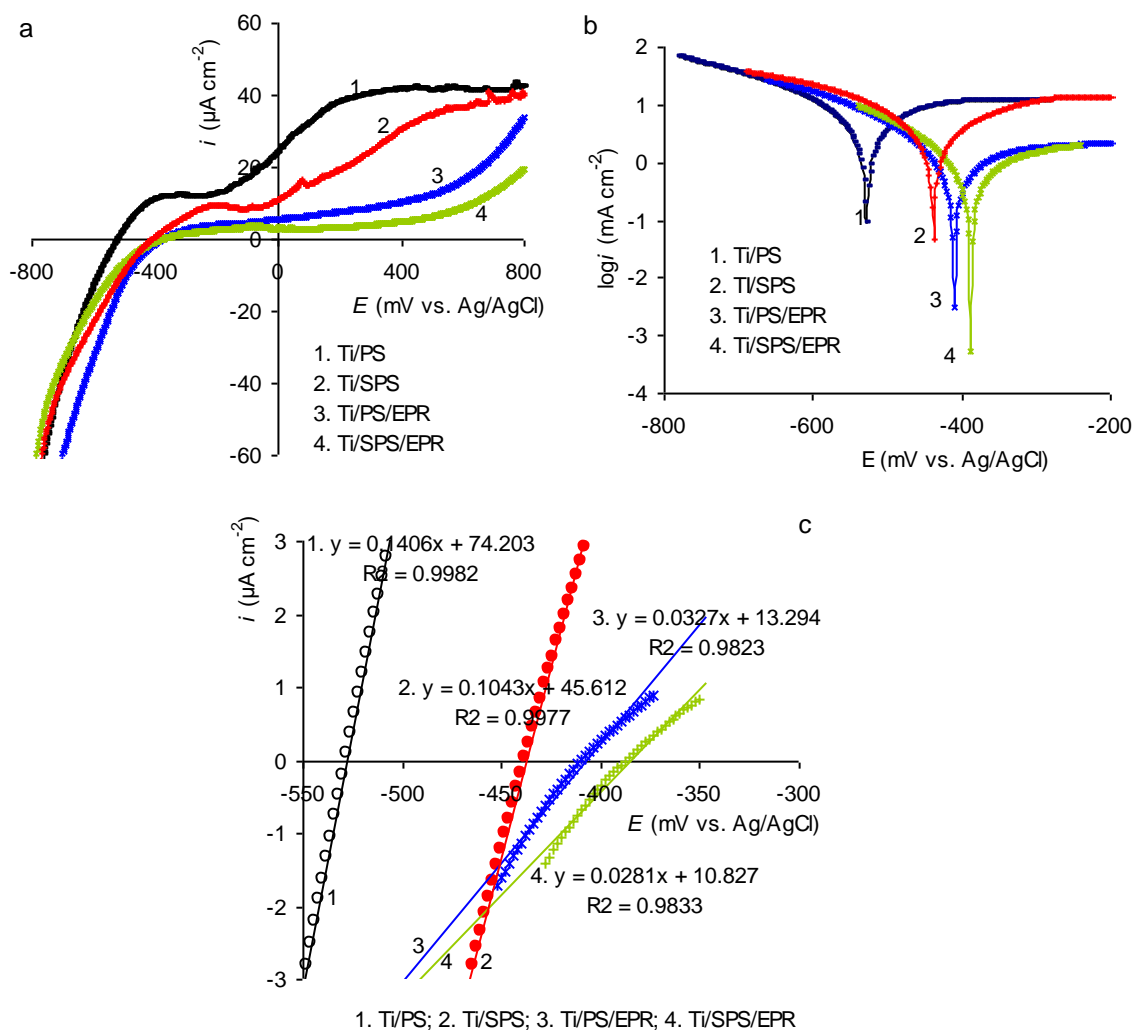


Figure 4. Electrochemical results for titanium electrode immersed in physiological serum blank and containing nAg/PVA in the absence and presence of epirubicin: a – potentiodynamic polarization curves; b - semilogarithmic curves; d – linear diagram

Thus, polarization resistance (R_p) was computed as: $R_p = 1/C_p$ [28, 29, 47]. The electrochemical parameters are listed in Table 1, as well as the protection performance (P%) assimilated to inhibition efficiency calculated as in other previous studies [28-30, 47] using the Equations 2, 3 and 4.

$$P = \frac{i_{corr}^o - i_{corr}}{i_{corr}^o} \times 100 \tag{2}$$

$$P = \frac{R_p - R_p^0}{R_p} \times 100 \quad (3)$$

$$P = \frac{CR^0 - CR}{CR^0} \times 100 \quad (4)$$

where: i_{corr}^0 , R_p^0 , CR^0 represent the corrosion current density, polarization resistance and corrosion rate ($\mu\text{m}/\text{year}$) obtained for the titanium corrosion in PS blank solution; i_{corr} , R_p and CR represent the corrosion current density, polarization resistance and corrosion rate, respectively computed for titanium corrosion in PS containing EPR, nAg/PVA and nAg/PVA/EPR, respectively.

Table 1. Electrochemical parameters of titanium immersed in physiological serum blank and containing nAg/PVA in the absence and presence of epirubicin

| Sample | E_{corr} / mV vs. Ag/AgCl | i_{corr} / $\mu\text{A cm}^{-2}$ | $C_p \cdot 10^3$ / S cm^{-2} | CR/ $\mu\text{m Y}^{-1}$ | R_p / $\text{k}\Omega \text{ cm}^2$ | | P/ % | | |
|------------|--|--|--|-----------------------------|---------------------------------------|--------------|---------------------------|---------------|------------|
| | | | | | from SlogC* | from LD** | from i_{corr} | from R_p | from CR |
| Ti/PS | -528 | 9.35 | 0.1406 | 162.9 | 7.19 | 7.11 | - | - | - |
| Ti/SPS | -438 | 6.63 | 0.1043 | 115.5 | 9.79 | 9.58 | 29.1 | 26.6 | 27.9 |
| Ti/PS/EPR | -410 | 1.58 | 0.0327 | 27.48 | 34.57 | 30.58 | 83.1 | 76.2 | 83.1 |
| Ti/SPS/EPR | -388 | 1.17 | 0.0281 | 20.1 | 38.6 | 35.58 | 87.5 | 81.3 | 87.6 |

*SlogC – semi-logarithmic curves

** LD – linear diagram

As can be seen from Table 1, the current density slightly drops and polarization resistance registered a small increase for Ti/SPS compared to Ti/PS, attaining a maximum value of 29.1% for protection performance. The epirubicin addition in physiological serum (Ti/PS/EPR) leads to a significant decrease of corrosion current and high value of polarization resistance, and consequently protection performance rises to 83.1%. As expected, the protection performance of EPR is slightly higher (max 87.6%) in the presence of nAg/PVA (Ti/SPS/EPR), confirming those above mentioned.

The results are in agreement with the other studies which reported that, the titanium exhibits relatively high corrosion resistance in the presence of Cl^- ions [45, 48, 49] and consequently, a low current density [45]. To retard titanium corrosion, organic compounds containing $-\text{NO}_2$ groups were investigated [50] as inhibitors leading to titanium polarization to more positive values.

3.3. Electrochemical impedance spectroscopy

Electrochemical impedance spectroscopy (EIS) is a suitable method to study the electrochemical processes at the metal/electrolyte interface, providing information on surface impedance modification. Taking into account that the impedance (Z) is a complex number composed

of a real part (Z_r - the resistance) and an imaginary part (Z_i - the reactance), it can be written according to Expression 5, where $j^2 = -1$ [51, 52]:

$$Z = Z_r + jZ_i \quad (5)$$

The complex admittance (Y) is related to the impedance according to Expression 6 [51], the conductance (Y_r) and the susceptance (Y_i) representing the real and imaginary part, respectively, as shown Expression 7 [51].

$$Y = 1/Z \quad (6)$$

$$Y = Y_r + jY_i \quad (7)$$

Consequently Nyquist diagram can be plotted according to impedance (Ny_Z) or admittance (Ny_Y), obtaining information on the resistance (Ohms) and conductance (Siemens), respectively. The both graphs are presented in Figure 5.

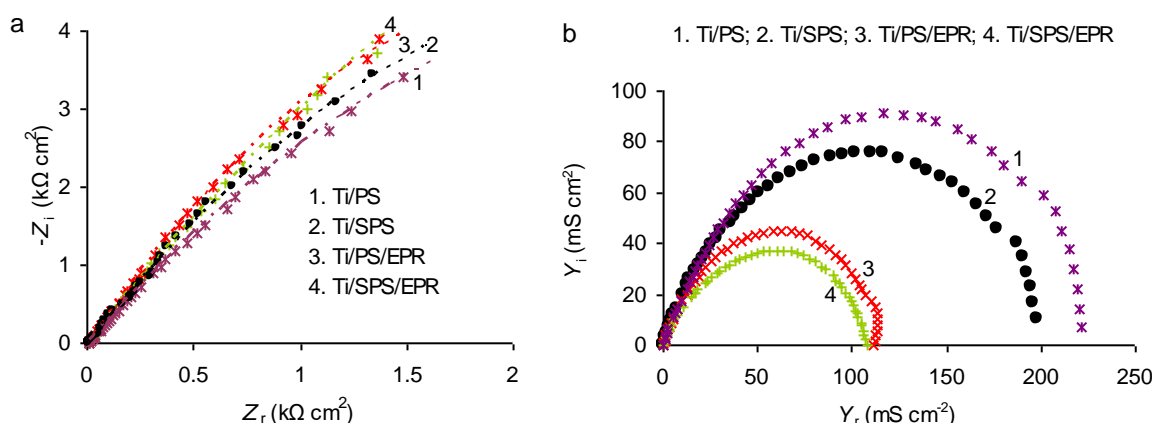


Figure 5. Nyquist plots recorded for titanium electrode immersed in physiological serum blank and containing nAg/PVA in the absence and presence of epirubicin: a – impedance representation detailed at high frequency range between 10^5 Hz and 10^2 Hz; b – admittance diagram

As shown in Fig. 5a, the Ny_Z diagram plotted between 10^5 Hz and 10^2 Hz displays capacitive loops with large diameters involving a great polarization resistance which apparently increases, as follows: Ti/PS < Ti/SPS < Ti/PS/EPR < Ti/SPS/EPR.

The Ny_Y diagram (Fig. 5b) shows capacitive loops with semicircle shapes more and more extensive with the decrease in admittance. The impedance/admittance measurements are in good agreement with the potentiodynamic polarization data, confirming the highest corrosion susceptibility for corroded titanium in PS (Ti/PS) and the highest resistance of titanium corroded in PS containing the nAg/PVA composite and epirubicin (Ti/SPS/EPR). Moreover, as well as the potentiodynamic measurements, the NY_Y diagram shows a distinctive titanium behavior in the presence of EPR (3), its effect being slightly stimulated by the nAg/PVA addition (4).

The experimental data fitting results, in the frequency range of 10^5 Hz and 10^{-1} Hz, presented in Figure 6 indicate many changes of interfacial architecture in the presence of nAg/PVA and EPR, especially revealed in the low frequency area, where more randomly dispersed points were recorded.

The best fitting of the experimental data was achieved using the equivalent circuit inserted in Figure 6. The equivalent circuit elements are represented by: the solution resistance (R_s); the coating

capacitance (C_{coat}); the coating resistance (R_{coat}); the double layer capacitance of the electrolyte at the metal surface (C_{dl}); the titanium polarization resistance (R_p) [46, 53]. The impedance electrochemical parameters are shown in Table 2.

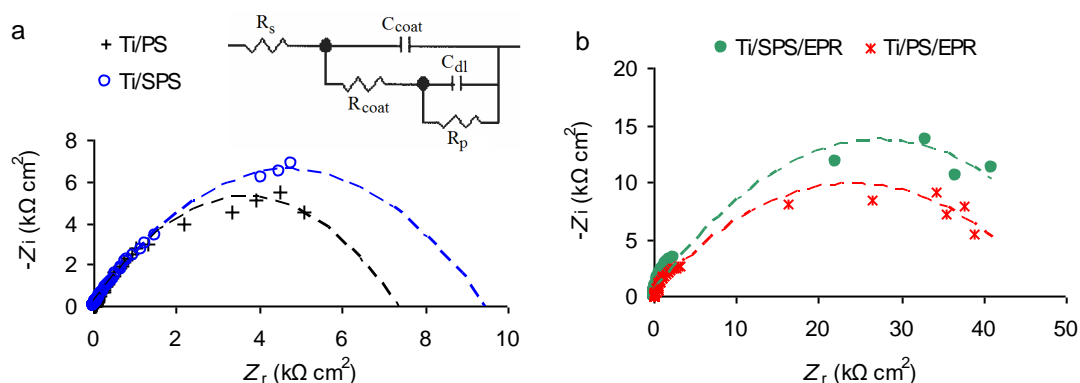


Figure 6. Nyquist diagrams for titanium electrode corroded in tested media: a – PS blank (Ti/PS) and PS containing nAg/PVA (Ti/SPS); b – PS containing EPR (Ti/PS/EPR) and PS containing nAg/PVA and EPR (Ti/SPS/EPR).

Table 2. Impedance parameters for titanium in physiological serum blank (Ti/PS) and containing: nAg/PVA (Ti/SPS); EPR (Ti/PS/EPR); nAg/PVA and EPR (Ti/SPS/EPR), at room temperature

| Sample | $R_s/$ $\text{m}\Omega \text{ cm}^2$ | $C_{\text{coat}}/$ $\mu\text{F cm}^{-2}$ | $R_{\text{coat}}/$ $\Omega \text{ cm}^2$ | $C_{\text{dl}}/$ $\mu\text{F cm}^{-2}$ | $R_p/$ $\text{k}\Omega \text{ cm}^2$ | P/ % |
|------------|---|---|---|---|---|------|
| Ti/PS | 593.3 | 2.15 | 4.4 | 534.6 | 7.18 | - |
| Ti/SPS | 563.2 | 2.01 | 4.9 | 487.3 | 9.87 | 27.2 |
| Ti/PS/EPR | 496.6 | 1.72 | 9.1 | 297.3 | 46.25 | 84.5 |
| Ti/SPS/EPR | 468.2 | 1.35 | 9.7 | 224.9 | 55.87 | 87.1 |

The R_{coat} , R_p , C_{coat} and C_{dl} evolution is due to an organic film assembling at the metal/electrolyte interface by the adsorption of inhibitors on the titanium surface [53]. The C_{coat} and C_{dl} variation might be associated with the dielectric constant decrease and/or to the thickness increase of the electrical double layer, revealing the occurrence of an adsorbed protective film on the titanium surface [53]. To calculate the layer protection performance, the Relationship 3 was employed. As can be seen from Table 2, the best protection is conferred by the nAg/PVA/EPR adsorbed layer, reaching a performance value of 87.1%, which is consistent with the data from potentiodynamic polarization.

3.4. Optical microscopy and AFM observation

Figures 7 and 8 display captured images from optical microscopy and AFM, respectively, for titanium surface corroded under the conditions mentioned in the previous paragraphs.

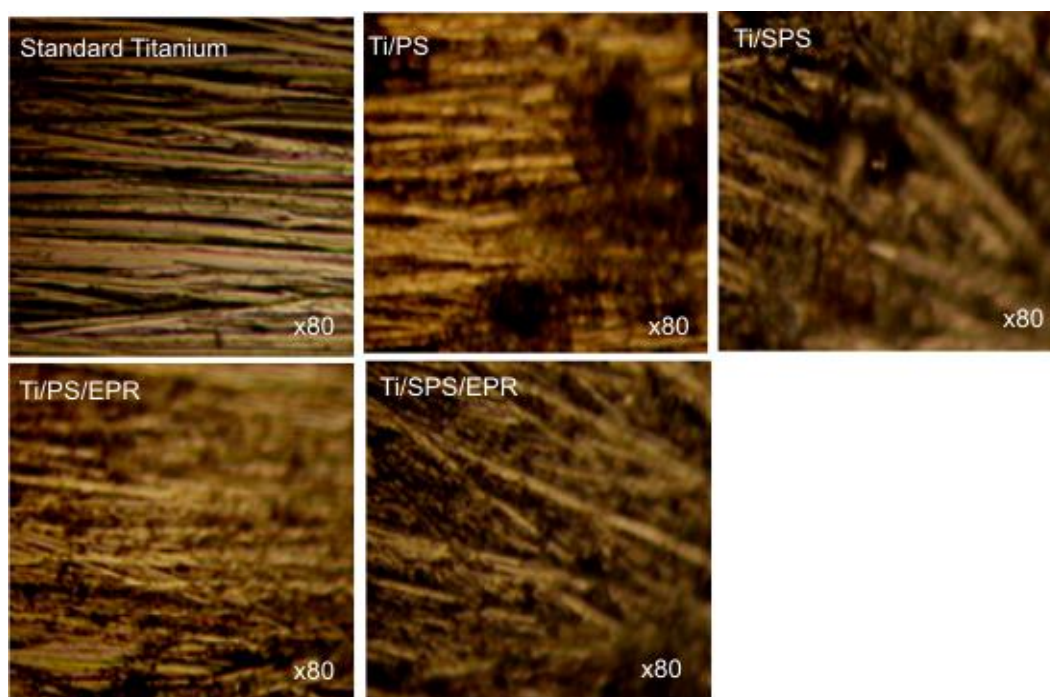


Figure 7. Optical microscopy images of titanium electrode before (Standard titanium) and after corrosion in: physiological serum (Ti/PS); in physiological serum containing nAg/PVA (Ti/SPS); in physiological serum containing epirubicin (Ti/PS/EPR) and physiological serum containing nAg/PVA and epirubicin (Ti/SPS/EPR)

After the titanium corrosion in PS, both methods design surface slides with a morphology affected by the presence of some randomly distributed spots (Fig. 7-Ti/PS), revealing a layer unevenness (Fig. 8a) that can not provides adequate protection. In the nAg/PVA presence, a well-defined film is observed on the surface, but with weakly adherence, leading to formation of anodic areas (Fig. 7-Ti/SPS) on which the corrosion processes can be intensified. Also, the histogram from Fig. 8b shows an irregular appearance with slightly arched sides, attesting to the fact that in the surface film some gaps that affect its continuity can occur.

The surface morphology from Fig. 7-Ti/ PS/ EPR shows a similar configuration to the standard and it can be assimilated with a classical surface modified by adsorption of some organic molecules which contributed to the protective layer development. The same information is provided by Fig. 8c where the film is disturbed by the presence of salt deposits on the upper-surface layer. Unlike Fig. 8a when the deposits are embedded in the layer, leading to its unevenness, in Fig. 8c most of them randomly appear on the surface without significantly altering of the coating Gaussian configuration revealed by the histogram (Fig. 8c).

The slide of Fig. 7-Ti/SPS/EPR shows a surface coated with a polymer film, but with a different configuration than that seen in Fig. 7_Ti/SPS. Moreover, the histogram regular shape having the largest width (Fig. 8d), indicates a relatively smooth film, apparently similar to the one presented in Fig. 8b. Note that there are certain salt free areas (Fig. 8d), whereon an evenly coating can be observed suggesting that the interaction between silver and epirubicin leads to an appropriate nAg/PVA/EPR

composite anchored by metal, especially by epirubicin adsorption or *via* epirubicin-bridges, which bind the silver nanoparticles adsorbed to PVA macromolecular chain from the titanium surface.

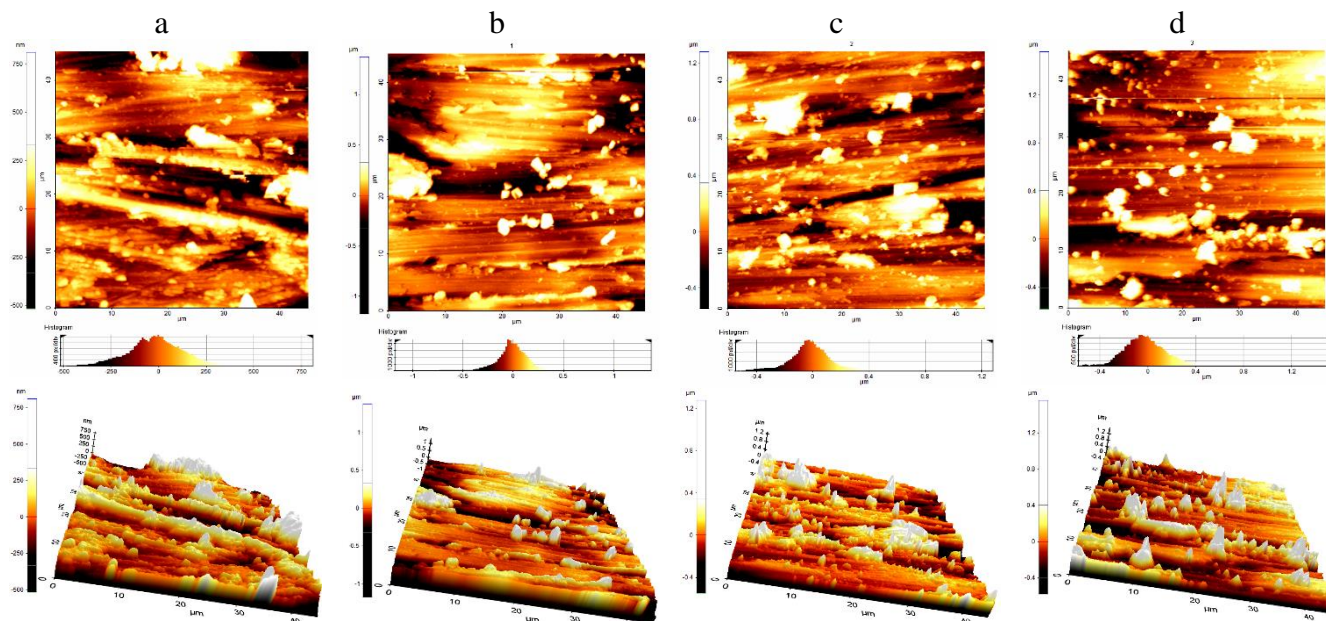


Figure 8. 2D and 3D AFM images of titanium electrode after corrosion in: a - physiological serum (Ti/PS); b - in physiological serum containing nAg/PVA (Ti/SPS); c - in physiological serum containing epirubicin (Ti/PS/EPR); d - physiological serum containing nAg/PVA and epirubicin (Ti/SPS/EPR)

4. CONCLUSIONS

The stable nAg/PVA nanodispersion was prepared and the kinetic model of nAg adsorption on PVA macromolecular chain was proposed. The nAg/PVA behaviour in the presence of Cl^- ions and the nAg-epirubicin interaction were emphasized.

The titanium surface modifications in physiological serum in the absence and presence of nAg/PVA and epirubicin were studied by electrochemical measurements associated with optical microscopy and atomic force microscopy (AFM). Unsatisfactory protection (performance of 29.1%) of the titanium surface was obtained in physiological serum containing just nAg/PVA caused by the slightly affinity of composite for titanium surface.

Epirubicin has a greater affinity for titanium due to the adsorption centers provided by oxygen and nitrogen atoms from its molecular structure ensuring a good surface protection of 83.1%. The nAg/PVA composite improves the performance of the cytostatic (87.6%) by facilitating its transport to the titanium/electrolyte interface and, in the same time, the silver-epirubicin interaction leads to a likely nAg/PVA/EPR composite bound on the substrate *via* epirubicin-bridges.

ACKNOWLEDGEMENT

The funding of this work was supported by the research grants awarded by the University of Craiova, Romania, in the competition “The Awards of Research Results-ISI Articles”, April 2017.

References

1. V. Kurowski and T. Wagner, *Cancer Chemoth. Pharm.*, 33 (1993) 36.
2. H. L. Donald, M. C. Kirk and R. F. Struk, *J. Che. Am. Soc.*, 92 (1970) 3207.
3. T. A. Connors, P. J. Farmer, P. B. Foster and A. B. Jarman, *Bioche. Pharmacol.*, 23 (1974) 115.
4. S. L. Cheeseman, S. P. Joel, J. D. Chester, G. Wilson, J. T. Dent, F. J. Richards and M. T. Seymour, *Brit. J. Cancer*, 87 (2002) 393.
5. M. L. Rothenberg, N.J. Meropol, E. A. Poplin, E. Van Cutsem and S Wadler, *J. Clin. Oncol.*, 18 (2001) 3801.
6. T. Andre, C. Louvet, F. Maindrault-Goebel, C. Couteau, M. Mabro, J. P. Lotz, V. Gilles-Amar, M. Krulik, E. Carola, V. Izrael and A. de Gramont, *Eur. J. Cancer*, 35 (1999) 1343.
7. Z. Bedzhova and G. Yordanov, *Colloid. Surface A*, 431 (2013) 27.
8. M. M. Abudabbusa, I. Jevremovića, K. Nešovića, A. Perić-Grujića, K. Y. Rhee and V. Mišković-Stanković, *Compos. Part B-Eng.*, 140 (2018) 99.
9. P. Sagitha, K. Sarada and K. Muraleedharan, *Trans. Nonferrous Met. Soc. China* 26 (2016) 2693.
10. I. M. Martinez Paino, *Enviro. Toxicol. Phar.*, 39 (2015) 614.
11. A. L. Potapova, O. A. Dainekoa, N. A. Ivanovaa, V. E. Agabekova and M. Bin-Hussainb, *Appl. Surf. Sci.*, 350 (2015) 121.
12. J. R. Bush, B. K. Nayak, L. S. Nair, M. C. Gupta and C. T. Laurencin, *J. Biomed. Mater. Res. B*, 97B (2011) 299.
13. T. R. Rautray and K.-H. Kim, *Mater. Technol.*, 25 (2010) 143;
<https://doi.org/10.1179/175355510X12723642365322>
14. A. Civantos, E. Martínez-Campos, V. Ramos, C. Elvira, A. Gallardo and A. Abarategi, *ACS Biomater. Sci. Eng.*, 3 (2017) 1245.
15. R. H. Oskouei, K. Fallahnezhad and S. Kuppusami, *Materials (Basel)*, 9 (2016) 111;
<https://doi.org/10.3390/ma9020111>
16. G. Wang and H. Zreiqat, *Materials*, 3 (2010) 3994.
17. A. Samide, I. Bibicu, M. Rogalsky and M. Preda, *Corros. Sci.*, 47 (2005) 1119.
18. I. Bibicu, A. Samide and M. Preda, *Mater. Lett.*, 58 (2004) 2650.
19. A. Samide, I. Bibicu, M. Rogalsky and M. Preda, *J. Radioanal. Nucl. Ch.*, 261(2004) 593.
20. B. V. Appa Rao and M. N. Reddy, *Arab. J. Chem.*, 10 (2017) S3270.
21. A. Samide, B. Tutunaru, Catalin Negrila and I. Prunaru, *Spectrosc. Lett.*, 45 (2012) 55.
22. A. Samide, *J. Environ. Sci. Heal. A*, 48 (2013) 159–165.
23. F. H. Stott, *J. Microscop.-Oxford*, 133; 1984: 191–204.
24. J. Arias, M. Cabeza, G. Castro, I. Feijoo, P. Merino and G. Pena, *J. Microscop.-Oxford*, 239 (2010) 184.
25. P. F. Khan, V. Shanthi, R. K. Babu, S. Muralidharan and R. C. Barik, *J. Environ. Chem. Eng.*, 3 (2015) 10.
26. A. Samide and B. Tutunaru, *J. Environ. Sci. Heal. A*, 46 (2011) 1713.
27. Y. Qiang, S. Zhang, Shenying Xu and W. Li, *J. Colloid. Interf. Sci.*, 472 (2016) 52.
28. A. Samide, G.E. Iacobescu, B. Tutunaru, R. Grecu, C. Tigae and C. Spînu, *Coatings*, 7 (2017) 181; <https://doi.org/10.3390/coatings7110181>
29. A. Samide, G. E. Iacobescu, B. Tutunaru and C. Tigae, *Int. J. Electrochem. Sci.*, 12 (2017) 2088.
30. A. Samide, B. Tutunaru, C. Ionescu, P. Rotaru and L. Simoiu, *J. Therm. Anal. Calorim.*, 118 (2014) 631.
31. J. Bontranger, A. Mahapatro and A.S. Gomez, *J. Microscop.-Oxford*, 255 (2014) 104.
32. A. Samide, B. Tutunaru, G. Bratulescu and C. Ionescu, *J. Appl. Polym. Sci.*, 130 (2013) 687.
33. T. Miller, J.-M. Lin, L. Pirolli, L. Coquilleau, R. Luharuka and A. V. Teplyakov, *Thin Solid Films*, 522 (2012) 193.
34. G. Tian, L. Dong, C. Wei, J. Huang, H. He and J. Shao, *Opt. Mater.*, 28 (2006) 1058.

35. A. Samide, R. Grecu, B. Tutunaru, C. Tigae and C. Spînu, *Int. J. Electrochem. Sci.*, 12 (2017) 11316.
36. A. Samide and B. Tutunaru, *Electroanal.*, 29(2017) 2498.
37. B. Tutunaru, A. Samide, C. Neamțu and C. Tigae, *Int. J. Electrochem. Sci.*, 13 (2018) 5850.
38. A. Sironmani and Ki. Daniel, *Silver Nanoparticles – Universal Multifunctional Nanoparticles for Bio Sensing, Imaging for Diagnostics and Targeted Drug Delivery for Therapeutic Applications in Drug Discovery and Development – Present and Future*, (2011) pp. 467, IntechOpen; doi: 10.5772/27047
39. U. Chatterjee, S. K. Jewrajka and S. Guh, *Polym. Compos.*, 30 (2009) 827.
40. Pandey, S. K. Pandey, V. Parashar, G. K. Mehrotra and A. C. Pandey, *J. Mater. Chem.*, 21 (2011) 17154.
41. L. Lu, A. Kobayashi, K. Tawa and Y. Ozaki, *Chem. Mater.*, 18 (206) 4894- 4901
42. N. A. Oladoja, C. O. Aboluwoye, and Y. B. Oladimeji, *Turkish J. Eng. Env. Sci.*, 32 (2008) 303.
43. D. M. Gligor and D. M. Măicăneanu, *Applications of Clay Minerals in Electrochemistry and Wastewater Treatment*, in “*Clay: Types, Properties and Uses*”, Editori: J.P.Humphrey, D.E. Boyd, Nova Science Publishers Inc., (2011) 1–61.
44. Z. Bedzhova and G. Yordanov, *Colloid. Surface A*, 431 (2013) 27.
45. Z. B. Wang, H. X. Hu and Y. G. Zheng, *Corros. Sci.*, 130 (2018) 203.
46. A. Samide, A. Ciuciu, C. Logofatu and M. Preda, *Mater. Plast.*, 47 (2010) 173.
47. A. Samide, P. Ilea and A. C. Vladu, *Int. J. Electrochem. Sci.*, 12 (2017) 5964.
48. J. Liu, A. Alfantazi and E. Asselin, *J. Electrochem. Soc.*, 162 (2015) C189.
49. G.T. Burstein and R.M. Souto, *Electrochim. Acta*, 40 (1995) 1881.
50. F.Mansfeld and J. V.Kenkel, *Corros. Sci.*, 15 (1975) 767.
51. K.S. Champlin, Method and apparatus for determining battery properties from complex impedance/admittance, US Patent 6222369B1 (2001). <https://patents.google.com/patent/US6222369B1/en>
52. Y. S. Lee, J.-H. Park, J. S. Choi and J. In Han, *Jpn. J. Appl. Phys.*, 42 (2003) 2715.
53. A. Samide, B. Tutunaru, C. Ionescu, C. Tigae and A. Moanță, *Int. J. Electrochem. Sci.*, 8 (2013) 3589.